J. Fluid Mech. (1994), *vol.* 279, *pp.* 197–215

Electrophoresis of slender particles

By YURI SOLOMENTSEV AND JOHN L. ANDERSON
Department of Chemical Engineering, Carnegie Mellon University, Pittsburgh, PA 15213, USA

(Received 17 February 1994 and in revised form 13 June 1994)

The hydrodynamic theory of slender bodies is used to model electrophoretic motion of a slender particle having a charge (zeta potential) that varies with position along its length. The theory is limited to systems where the Debye screening length of the solution is much less than the typical cross-sectional dimension of the particle. A stokeslet representation of the hydrodynamic force is combined with the Lorentz reciprocal theorem for Stokes flow to develop a set of linear equations which must be solved for the components of the translational and angular velocities of the particle. Sample calculations are presented for the electrophoretic motion of straight spheroids and cylinders and a torus in a uniform electric field. The theory is also applied to a straight uniformly charged particle in a spatially varying electric field. The uniformly charged particle rotates into alignment with the principal axes of $\nabla \boldsymbol{E}_\infty$; we suggest that such alignment can lead to electrophoretic transport of particles through a small aperture in an otherwise impermeable wall. The theory developed here is more general than just for electrophoresis, since the final result is expressed in terms of a general 'slip velocity' at the surface of the particle. Thus, the results are applicable to diffusiophoresis of slender particles if the proper slip-velocity coefficient is used.

1. Introduction

Phoretic processes are characterized by localization of the driving forces in a boundary layer near the surface of a particle suspended in a fluid (Anderson 1989). In electrophoresis the particle moves because the applied electric field exerts a force on the electrical double layer at the surface. The thickness of the boundary layer is of order of the Debye screening length of the solution (κ^{-1}); typical values of κ^{-1} in aqueous solutions are 10–100 Å. Generally the particle size exceeds the Debye screening length; this includes a broad range of colloidal species from large biomolecules to inorganic particles such as clay.

There is a considerable literature on the theory of electrophoresis (for example, Hunter 1981; Dukhin & Derjaguin 1974; O'Brien & White 1978; Saville 1977; O'Brien 1983). While most of this work has been concerned with steady external electric fields, electrophoresis in high-frequency fields has been modelled (O'Brien 1990; Mangelsdorf & White 1992). The basic physical model is a spherical particle of radius R having a uniform electrostatic potential, called the 'zeta potential' (ζ), on the surface. The zeta potential is related to the charge per unit area of the surface through models for the double layer. The electrophoretic mobility, defined as the particle's velocity divided by the applied electric field, depends on κR and ζ. The electrophoresis of uniformly charged spheroids has also been modelled when the zeta potential is about kT/e or less (Yoon & Kim 1989) or when the zeta potential is arbitrarily large but the Debye screening length is small relative to particle dimensions (O'Brien & Ward 1988).

Nature is not always obliging and offers colloidal species that are non-uniformly

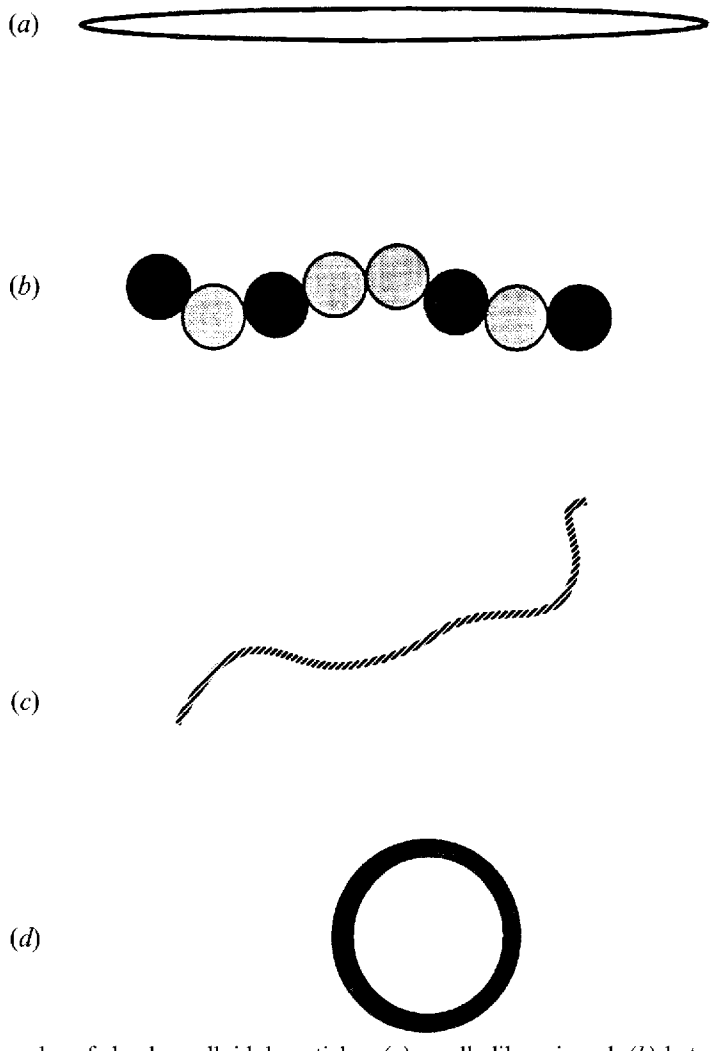

FIGURE 1. Examples of slender colloidal particles: (*a*) needle-like mineral, (*b*) heteroaggregate of simple particles, (*c*) charged polymer chain or bundle of chains, (*d*) torus (e.g. DNA plasmid).

charged and non-spherical. Hydrodynamic theories for non-uniformly charged particles have been developed over the past decade. The geometries considered thus far include spheres (Anderson 1985; Yoon 1991; Solomentsev, Pawar & Anderson 1993), general ellipsoids (Fair & Anderson 1989), and chains of spheres (Fair & Anderson 1990; Keh & Yang 1991). The interesting results from these analyses include the following: even moments of ζ cause a non-isotropic mobility, which means the magnitude and direction of the particle's velocity is a function of its orientation with respect to the applied electric field; odd moments of ζ lead to alignment of the particle with the applied field; and a neutral particle can have a significant electrophoretic velocity. Some of these predictions have been observed with aggregates of colloidal spheres (Fair 1990; Fair & Anderson 1992; Pawar 1993).

In this paper we consider slender particles that have an arbitrary distribution of ζ along their contours. Examples of colloidal structures that might be modelled by slender-body theory are shown in figure 1. Theories for Stokes flow about slender bodies have been developed to various degrees of approximation (Batchelor 1970; Cox

1970; Keller & Rubinow 1976; Johnson & Wu 1979; Johnson 1980). In the next section we combine the concept of 'slip velocity', which arises in phoretic processes (Anderson 1989), with a stokeslet representation of the stress on a slender particle to obtain relations between the velocity of the particle and the variation of the slip velocity along the centreline of the particle. Use is made of the Lorentz reciprocal theorem for Stokes flow and the zero-force and zero-couple constraints that apply to phoretic transport to obtain a set of algebraic equations (see (2.13)) that must be solved for the components of the translational and angular velocities of the particle. Some examples of different particle geometries (contours) are considered in §3 to demonstrate the application of the theory to electrophoresis. In §4 the theory is applied to a uniformly charged straight particle in an electric field that varies with position. The result is used to estimate the field required to align straight particles in converging electric field lines at the entrance of a small hole in a plane wall.

2. General model

2.1. *Slip velocity*

Electrokinetic phenomena result from stresses on the charge double layer at a solid/liquid interface. The double layer consists of a 'fixed charge' on the surface and a diffuse 'space charge' in the adjoining liquid. The space charge balances the fixed charge, so that the entire double layer is neutral. The simplest theory for the charge distribution in the equilibrium double layer is the Gouy–Chapman model (Hunter 1981; Russel, Saville & Schowalter 1989) which treats the free ions in the liquid as point charges and considers the fixed charge at the solid interface to be 'smeared' into a continuum. Even with its simplifying assumptions, the Gouy–Chapman model gives results for the distribution of space charge that agree well with more rigorous theories based on the statistical mechanics of finite-size ions and solvent molecules.

An important parameter of the double layer is the Debye screening length, κ^{-1}, which is inversely proportional to the square root of the electrolyte concentration in the solution; for 0.1 molar sodium chloride in water at room temperature, $\kappa^{-1} = 9.6$ Å. At distances (y) greater than κ^{-1} from a planar surface, the space-charge density and the double-layer potential both decay to zero as $\exp(-\kappa y)$. This exponential decay is important when modelling electrokinetic flows in unbounded fluids because the charge on the solid surface is essentially screened for y greater than several values of κ^{-1}.

The term 'electro-osmosis' refers to electrokinetic flow past a stationary charged solid when an electric field is applied. An electric field originating from an external source exerts a body force on the space charge which is transmitted to the liquid within the double layer ($y \sim O(\kappa^{-1})$). The velocity field is described by the Stokes equations including this electrical force. The general description of electrokinetics ignores second-order charge effects, such as media polarization which would introduce terms of $O(E^2)$ (Melcher 1981). If the radius of curvature of the solid is much larger than κ^{-1} then the space charge is not distorted and the electro-osmotic velocity is parallel to the solid surface in the direction of the tangential field, $\boldsymbol{E}^s$. By using Poisson's equation to relate the space charge to the variation in electrostatic potential and integrating the Stokes equation for one-dimensional flow across the double layer, one obtains the Helmholtz equation for the electro-osmotic 'slip velocity' $\boldsymbol{u}$:

$$\kappa y \gg 1: \quad \boldsymbol{v} \to \boldsymbol{u} = -\frac{D}{\eta}\left(\frac{kT}{e}\right)\zeta \boldsymbol{E}^s. \tag{2.1}$$

ζ is the 'zeta potential' normalized by the thermal potential kT/e, and D and η are the permittivity and viscosity of the liquid. The term $[DkT/\eta e]$ equals 1.80 (μm s^{-1})/(volt cm^{-1}) for water at 20 °C. On a lengthscale characteristic of the particle's geometry, which is much greater than κ^{-1}, the conventional 'no-slip' condition on the velocity field at the particle's surface is relaxed and the fluid moves at a velocity $\boldsymbol{u}$ relative to the solid surface. Note that osmotic flows, which result from solute concentration gradients along a surface, can also lead to a slip velocity (Anderson 1989).

When considering the hydrodynamics of electrophoresis, (2.1) forms the inner boundary condition for flow outside the double layer. The concept of slip velocity is very useful for describing the hydrodynamics of electrophoresis and other electrokinetic transport processes when κ^{-1} is much smaller than the radius of curvature of the solid surface (Anderson 1989; Acrivos, Jeffrey & Saville 1990). If the particle is uniformly charged with zeta potential ζ_0 and if $(\kappa R)^{-1}[\exp(|\zeta_0|/2)-1] \ll 1$ at all positions on the surface, where R is the mean radius of curvature, then the translational ($\boldsymbol{U}$) and angular ($\boldsymbol{\Omega}$) velocities are given by the following no matter what the shape or orientation of the particle as long as the applied electric field ($\boldsymbol{E}_\infty$) is independent of position:

$$\left.\begin{aligned} \boldsymbol{U} &= \left(\frac{DkT}{\eta e}\right)\zeta_0 \boldsymbol{E}_\infty, \\ \boldsymbol{\Omega} &= \boldsymbol{0}. \end{aligned}\right\} \tag{2.2}$$

The above relation for $\boldsymbol{U}$ is attributed to Smoluchowski (Hunter 1981).

If κ^{-1} is comparable to the radius of curvature of a particle, (2.2) is no longer correct and the particle's velocity is a function of particle size and shape. References are made in the previous section to theories for spherical and spheroidal particles having finite κR. The effect of finite κR for long straight cylinders of radius R has also been examined. Henry (1931) considered particles with $|\zeta_0|$ of order 1 or less and arbitrary κR but very large κL, where L is the half-length of the cylinder. The coefficient relating the cylinder's translational velocity to the applied field is no longer a scalar as shown in (2.2), rather it has different components for the directions parallel and perpendicular to the axis of the cylinder. Sherwood (1982) extended the analysis to cases where $\kappa R \ll 1$ but κL is arbitrary. Keh & Chen (1993) considered the case $\kappa R \gg 1$ and found that the electrophoretic mobility for the applied field directed perpendicular to the cylinder's axis depends on the parameter $\lambda = 2(\kappa R)^{-1}[\exp(|\zeta_0|/2)-1]$ in the same way as the mobility of a uniformly charged sphere of the same radius (Dukhin & Derjaguin 1974).

We will not take into account these more sophisticated analyses of the electrokinetics of cylinders in our hydrodynamic model for slender bodies, as described below, because we require $\kappa b_0 \gg \ln \epsilon^{-1}$ where b_0 is the radius of the slender body and ϵ is the slenderness parameter. Therefore, we rely on (2.1) to provide the inner boundary condition for the velocity field outside the double layer.

2.2. *Hydrodynamic model*

The configuration of the slender particle is shown in figure 2. It is assumed to be a rigid body. The length is $2L$ and the maximum radius is b_0; the slenderness parameter (ϵ) is defined as b_0/L and is assumed to be small. The cross-section is locally cylindrical with a radius b which is a function of the position along the contour (s) which is made dimensionless by L. The centreline of the particle is specified by the vector function $\boldsymbol{X}_0(s)$; it may be curved as long as the radius of curvature is $O(L)$. A local orthonormal

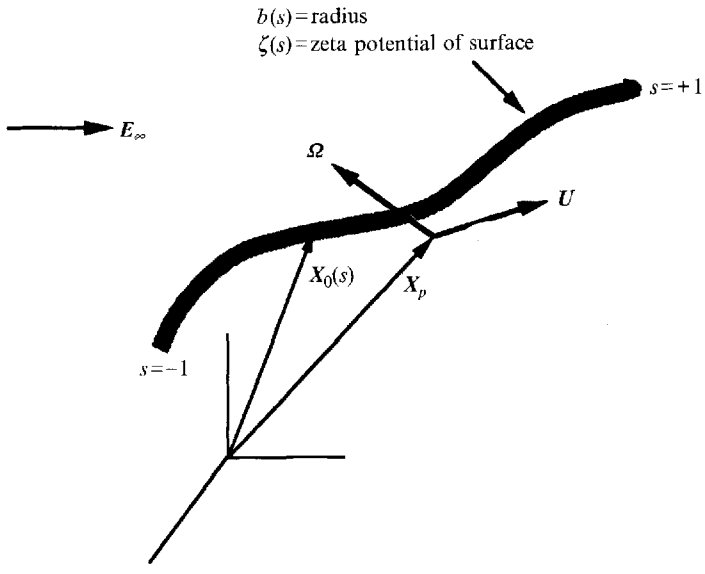

FIGURE 2. General slender body. The centre of the particle (X_p) is not necessarily at the centre of the contour ($s = 0$).

set of unit vectors at each centreline position is defined with e_t parallel to the line that is tangent to the contour:

$$e_t = \frac{\mathrm{d}X_0}{L\,\mathrm{d}s}, \quad e_n = \frac{1}{L^2 H}\frac{\mathrm{d}^2 X_0}{\mathrm{d}s^2}, \quad e_b = e_t \times e_n, \tag{2.3}$$

where H is the curvature of the particle's contour. If the centreline is straight then e_n is chosen to be in the direction of $(I - e_t e_t)\cdot E$ where I is the unit dyadic and E is the local electric field.

U is the translational velocity of the centre of the particle, which is not necessarily the point $s = 0$, and Ω is the angular velocity. We assume that the double-layer thickness, which is of the order of the Debye screening length of the solution (κ^{-1}), is much smaller than b_0. U and Ω are determined by requiring the hydrodynamic force and couple on the particle to equal zero. Outside the double layer the velocity field is described by the Stokes equations with no electrical body force term

$$\eta\nabla^2 v - \nabla p = 0; \quad \nabla\cdot v = 0. \tag{2.4}$$

The electrodynamics are incorporated into the problem by specifying the slip velocity u as a function of position s along the centreline. A boundary S^+ is defined to enclose the particle and its double layer; thus, S^+ is displaced from the true surface of the particle (S^p) by a distance of $O(\kappa^{-1})$. The boundary conditions on the velocity field described by (2.4) are:

$$\text{on} \quad S^+: \quad v = U + \Omega \times r + u(s), \tag{2.5a}$$

$$r \to \infty: \quad v \to 0, \tag{2.5b}$$

where U and Ω are the (unknown) translational and angular velocities of the particle. In the case of electrophoresis u is given by (2.1); however, we shall develop the hydrodynamic model for arbitrary u so that the result applies to any phoretic motion for which the interfacial thickness, such as the double layer, is small relative to the radius of the particle. The unknown velocities U and Ω are determined by setting the hydrodynamic force and couple on S^+ equal to zero.

For a slender particle the surface $S^+ \approx S^p$ is approximated by $\boldsymbol{R}(s) = \boldsymbol{X}_0(s) - \boldsymbol{X}_p$ where $\boldsymbol{X}_p$ is the position of the 'centre' of the particle. The velocity field is split into two contributions: $\boldsymbol{v}^h$ = the velocity in the absence of a slip velocity ($\boldsymbol{u} = \boldsymbol{0}$) with $\boldsymbol{U}$ and $\boldsymbol{\Omega}$ specified; and $\boldsymbol{v}^e$ = the electrokinetic velocity that satisfies (2.4) and (2.5) with both $\boldsymbol{U}$ and $\boldsymbol{\Omega}$ equal to $\boldsymbol{0}$ but $\boldsymbol{u}$ an arbitrary function of s. The zero force and couple constraints are

$$\iint_{S^+} \boldsymbol{n}\cdot\boldsymbol{\sigma}^e \,\mathrm{d}S = -\iint_{S^+} \boldsymbol{n}\cdot\boldsymbol{\sigma}^h \,\mathrm{d}S, \tag{2.6a}$$

$$\iint_{S^+} \boldsymbol{r}\times(\boldsymbol{n}\cdot\boldsymbol{\sigma}^e)\,\mathrm{d}S = -\iint_{S^+} \boldsymbol{r}\times(\boldsymbol{n}\cdot\boldsymbol{\sigma}^h)\,\mathrm{d}S, \tag{2.6b}$$

where $\boldsymbol{n}$ is the unit normal pointing from S^+ into the surrounding fluid and $\boldsymbol{\sigma}$ is the stress dyadic for a Newtonian fluid. $\boldsymbol{U}$ and $\boldsymbol{\Omega}$ are determined by satisfying (2.6).

The electrodynamic problem ($\boldsymbol{v}^e$) is now circumvented by applying the Lorentz reciprocal theorem (Happel & Brenner 1973) to the fluid outside S^+. Since there are no body forces in this region (i.e. $\nabla\cdot\boldsymbol{\sigma}^e = \boldsymbol{0}$) and all velocities approach zero far from S^+, we have

$$\iint_{S^+} \boldsymbol{n}\cdot\boldsymbol{\sigma}^e\cdot\boldsymbol{v}^* \,\mathrm{d}S = \iint_{S^+} \boldsymbol{n}\cdot\boldsymbol{\sigma}^*\cdot\boldsymbol{v}^e \,\mathrm{d}S, \tag{2.7}$$

where $\boldsymbol{v}^*$ is the velocity that satisfies (2.4) and (2.5) with $\boldsymbol{u} = \boldsymbol{0}$ and $(\boldsymbol{U}, \boldsymbol{\Omega})$ replaced by the constant but arbitrary vectors $(\boldsymbol{U}^*, \boldsymbol{\Omega}^*)$. On S^+ the electrodynamic velocity equals $\boldsymbol{u}(s)$. The value of $\boldsymbol{v}^*$ on S^+ is approximated by the following for a slender body:

$$\text{on } S^+\text{:}\quad \boldsymbol{v}^* \approx \boldsymbol{U}^* + \boldsymbol{\Omega}^*\times\boldsymbol{R}(s). \tag{2.8}$$

Combining the above two relations gives

$$\iint_{S^+} \boldsymbol{n}\cdot\boldsymbol{\sigma}^e\cdot[\boldsymbol{U}^* + \boldsymbol{\Omega}^*\times\boldsymbol{R}(s)]\,\mathrm{d}S = \iint_{S^+} \boldsymbol{n}\cdot\boldsymbol{\sigma}^*\cdot\boldsymbol{u}(s)\,\mathrm{d}S. \tag{2.9}$$

Finally, we use (2.6) to eliminate the electrodynamic stress. The result is

$$\iint_{S^+} \boldsymbol{n}\cdot\boldsymbol{\sigma}^h \,\mathrm{d}S\cdot\boldsymbol{U}^* + \iint_{S^+} \boldsymbol{R}(s)\times(\boldsymbol{n}\cdot\boldsymbol{\sigma}^h)\,\mathrm{d}S\cdot\boldsymbol{\Omega}^* = -\iint_{S^+} \boldsymbol{n}\cdot\boldsymbol{\sigma}^*\cdot\boldsymbol{u}(s)\,\mathrm{d}S, \tag{2.10}$$

$\boldsymbol{\sigma}^h$ and $\boldsymbol{\sigma}^*$ are linear functions of $(\boldsymbol{U}, \boldsymbol{\Omega})$ and $(\boldsymbol{U}^*, \boldsymbol{\Omega}^*)$. The above expression provides six scalar equations, one for each of the arbitrary components of $\boldsymbol{U}^*$ and $\boldsymbol{\Omega}^*$, which must be solved to obtain the electrophoretic velocities $\boldsymbol{U}$ and $\boldsymbol{\Omega}$.

The stress along the surface of the particle can be expressed in terms of a distribution of stokeslets $\boldsymbol{\alpha}^i(s)$. For the hydrodynamic flow we write the stress per unit length as

$$b(s)\int_{s=\text{constant}} \boldsymbol{n}\cdot\boldsymbol{\sigma}^h \,\mathrm{d}\phi = -8\pi\eta\sum_{i=1}^{6} \boldsymbol{\alpha}^i(s)\, V_i, \tag{2.11}$$

where ϕ is the polar angle about the centreline axis at fixed s. Note that $V_i = U_i$ for $i = 1\to 3$ and $V_i = \Omega_{i-3}$ for $i = 4\to 6$. Equation (2.11) also holds for the arbitrary-flow problem with $\boldsymbol{\sigma}^h$ replaced by $\boldsymbol{\sigma}^*$ and V_i by V_i^*. The force and torque on S^+ for the purely hydrodynamic part of the problem are

$$\boldsymbol{F}^{(h)} = -8\pi\eta L\sum_{i=1}^{6} V_i\int_{-1}^{+1} \boldsymbol{\alpha}^i(s)\,\mathrm{d}s, \quad \boldsymbol{T}^{(h)} = -8\pi\eta L\sum_{i=1}^{6} V_i\int_{-1}^{+1} \boldsymbol{R}(s)\times\boldsymbol{\alpha}^i(s)\,\mathrm{d}s. \tag{2.12}$$

After combining (2.10) and (2.11) and expressing the result in Cartesian components, we have the following equations which must be solved for the 6 components of V_i, the first three being $\boldsymbol{U}$ and the second three being $\boldsymbol{\Omega}$:

$$\left.\begin{aligned} &m = 1,2,3: \quad V_i \int_{-1}^{+1} \alpha_m^i(s)\,\mathrm{d}s = -\int_{-1}^{+1} \alpha_p^m(s)\,u_p(s)\,\mathrm{d}s, \\ &m = 4,5,6: \quad \epsilon_{jkn}\,V_i \int_{-1}^{+1} R_j(s)\,\alpha_k^i(s)\,\mathrm{d}s = -\int_{-1}^{+1} \alpha_p^m\,u_p(s)\,\mathrm{d}s, \\ &(n = m-3) \end{aligned}\right\} \tag{2.13}$$

where ϵ_{jkn} is the permutation tensor. The standard summation convention is used for repeated indices, with i over $1 \to 6$ and (p,j,k) over $1 \to 3$. The general problem for phoretic motion of slender bodies, when the interfacial layer is thin relative to the radius, has been reduced to solving the six equations in (2.13). Application of this result depends on the model for the slip velocity $\boldsymbol{u}$.

One might question why we apply the reciprocal theorem at S^+, instead of at S as was done by Sherwood (1982) and Teubner (1982). The reason for choosing S^+ is that we avoid the volume integral of the electrical stresses over the double-layer region. Evaluation of this integral would require knowledge of the field variables (electrostatic potential, velocity) within the double layer, which means the theory would be model specific and considerably more effort would be required to evaluate the particle's velocity than simply solving (2.13). In our approach the only information needed is the stokeslet distributions for translation and rotation of the slender particle and the slip velocity which is proportional to the field outside the double layer; of course, the coefficient of this proportionality depends on the model for the dynamics within the double layer. The disadvantage of our approach is that the results are valid only when $\kappa b_0 \gg 1$, as discussed in §5.

2.3. *Determination of the stokeslets*

Several theories are available for determining the stokeslet distributions for a general centreline profile $\boldsymbol{X}_0(s)$ and cross-section radius $b(s)$ (Batchelor 1970; Cox 1970; Keller & Rubinow 1976; Johnson 1980). While Johnson's theory is, in principle, accurate to $O(\epsilon^2 \ln \epsilon)$, it has the disadvantage of requiring the solution of an integral equation. Cox (1970) neglected the ends and derived an explicit method for calculating the stokeslet distribution to $O((\ln \epsilon)^{-2})$ for a general centreline profile, as long as the radius of curvature of the profile is much greater than b_0. Cox's result can be derived from Johnson's model by expanding $\boldsymbol{\alpha}$ in powers of $(\ln \epsilon)^{-1}$. For the examples given in the next section, we use Cox's method to compute the stokeslets needed to solve (2.13), except for the toroidal ring and the prolate spheroid because analytical results are available with error of $O(\epsilon^2 \ln \epsilon)$.

In general six stokeslet functions, $\boldsymbol{\alpha}^i(s)$, are needed, one for each component of $\boldsymbol{U}^*$ and $\boldsymbol{\Omega}^*$. Equations (6.2) and (6.3) of Cox (1970) can be expressed as

$$4\boldsymbol{\alpha}^i = \frac{1}{\ln \epsilon}\,\boldsymbol{W}^i \cdot [2\boldsymbol{I} - \boldsymbol{e}_t \boldsymbol{e}_t] + \left(\frac{1}{\ln \epsilon}\right)^2 \{\tfrac{1}{2}\boldsymbol{W}^i \cdot [2\boldsymbol{I} - 3\boldsymbol{e}_t \boldsymbol{e}_t] + \boldsymbol{Y}^i \cdot [2\boldsymbol{I} - \boldsymbol{e}_t \boldsymbol{e}_t]\}. \tag{2.14}$$

The fluid velocity far from the particle is zero and $\boldsymbol{W}^i$ is the velocity of point s along the contour:

$$\left.\begin{aligned} &\text{(translation)}\ i = 1 \to 3: \quad W_j^i = \delta_{ij}, \\ &\text{(rotation)} \quad i = 4 \to 6: \quad W_j^i = \epsilon_{i-3,nj} R_n(s), \end{aligned}\right\} \tag{2.15}$$

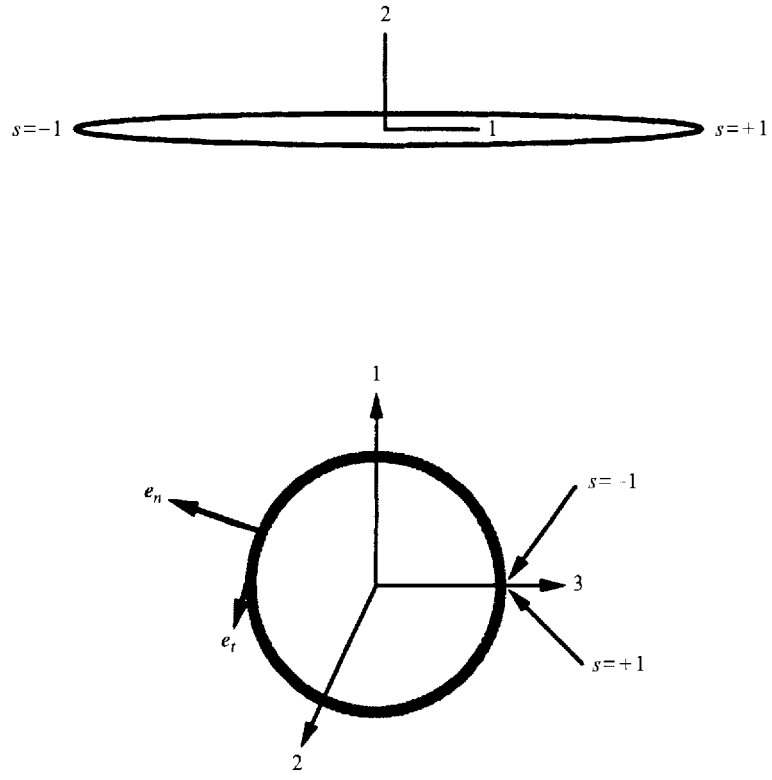

FIGURE 3. Coordinate definitions for straight particle and torus. The origin of the local coordinate system is at the centre of the particle. The torus lies in the 1–3 plane.

δ_{ij} is the unit tensor, ϵ_{inj} is the permutation operator and the index 'j' denotes one of the three fixed Cartesian directions. The function $\boldsymbol{Y}^i$ accounts for effects of velocity disturbances originating from distant positions (s') along the contour:

$$\boldsymbol{Y}^i(s) = \ln\left(\frac{2\beta}{w(s)}\right)\boldsymbol{W}^i(s)$$

$$-\frac{1}{2}\left[\int_0^{s-\beta} \mathrm{d}s' + \int_{s+\beta}^{1} \mathrm{d}s'\right]\left\{\left[\frac{1}{|\boldsymbol{R}-\boldsymbol{R}'|}\boldsymbol{I} + \frac{1}{|\boldsymbol{R}-\boldsymbol{R}'|^3}(\boldsymbol{R}-\boldsymbol{R}')(\boldsymbol{R}-\boldsymbol{R}')\right]\cdot[\boldsymbol{I}-\tfrac{1}{2}\boldsymbol{e}_t'\boldsymbol{e}_t']\cdot\boldsymbol{W}^i(s')\mathrm{d}s'\right\}, \tag{2.16}$$

where the primed quantities ($'$) denote a function of s' and w is the dimensionless radius ($= b(s)/b_0$). The parameter β is arbitrarily small and is included to avoid a singular integral; it is eliminated upon performing the integration.

The results of applying (2.14)–(2.16) to a straight cylinder are (see figure 3 for coordinates):

$$\alpha_1^1 = \frac{1-2\ln(2\epsilon(1-s^2)^{1/2})}{8(\ln\epsilon)^2}, \quad \alpha_2^2 = \frac{1+2\ln(2\epsilon(1-s^2)^{1/2})}{4(\ln\epsilon)^2}, \quad \alpha_2^6 = \frac{s[1-2\ln(2\epsilon(1-s^2)^{1/2})]}{4(\ln\epsilon)^2}. \tag{2.17}$$

The subscript is the direction of the force and the superscript is the component of velocity (U_i for $i = 1 \to 3$ and Ω_{i-3} for $i = 4 \to 6$). To check the accuracy of Cox's model,

we consider a cylinder with $\epsilon = 0.1$. In figure 4 we compare the stokeslet distribution for translation parallel to the cylinder's axis (α_1^1) as determined from (2.17) to the stress found from numerical solution of the Stokes equations using the software FLUENT® (CREARE.X, Inc., Hanover, New Hampshire). The agreement appears good.

For a prolate spheroid the stokeslet functions α_1^1 and α_2^2 are constants and $\alpha_2^6 \sim s$, to $O(\epsilon^2 \ln \epsilon)$. These values are (Johnson 1980):

$$\alpha_1^1 = \frac{1}{2\left[2\ln\left(\frac{2}{\epsilon}\right)-1\right]}, \quad \alpha_2^2 = \frac{1}{2\ln\left(\frac{2}{\epsilon}\right)+1}, \quad \alpha_2^6 = \frac{s}{2\ln\left(\frac{2}{\epsilon}\right)-1}. \tag{2.18}$$

Johnson & Wu (1979) derived the following for a torus:

$$\left.\begin{aligned}
\boldsymbol{\alpha}^1 &= \frac{-3+\ln(8/\gamma)}{-2-5\ln(8/\gamma)+2\ln^2(8/\gamma)}\sin[\pi(1+s)]\,\boldsymbol{e}_n \\
&\quad + \frac{-5+2\ln(8/\gamma)}{-8-20\ln(8/\gamma)+8\ln^2(8/\gamma)}\cos[\pi(1+s)]\,\boldsymbol{e}_t, \\
\boldsymbol{\alpha}^2 &= \frac{1}{1+2\ln(8/\gamma)}\boldsymbol{e}_b, \\
\boldsymbol{\alpha}^3 &= \frac{-3+\ln(8/\gamma)}{2+5\ln(8/\gamma)-2\ln^2(8/\gamma)}\cos[\pi(1+s)]\,\boldsymbol{e}_n \\
&\quad + \frac{-5+2\ln(8/\gamma)}{-8-20\ln(8/\gamma)+8\ln^2(8/\gamma)}\sin[\pi(1+s)]\,\boldsymbol{e}_t, \\
\boldsymbol{\alpha}^4 &= \frac{1}{-3+2\ln(8/\gamma)}\cos[\pi(1+s)]\,\boldsymbol{e}_b, \\
\boldsymbol{\alpha}^5 &= \frac{1}{-8+4\ln(8/\gamma)}\boldsymbol{e}_t, \\
\boldsymbol{\alpha}^6 &= \frac{1}{-3+2\ln(8/\gamma)}\sin[\pi(1+s)]\,\boldsymbol{e}_b,
\end{aligned}\right\} \tag{2.19}$$

where $\gamma = \pi\epsilon$.

2.4. *Electrophoretic motion*

The determination of the slip velocity requires the electric field at each point s along the centreline. Cole (1968) has shown that for a slender particle in a potential field that obeys Laplace's equation, the local gradient of the potential on the scale of L equals the undisturbed potential if terms of $O(\epsilon^2 \ln \epsilon)$ are neglected. Therefore, the 'applied field' felt by a local segment of the particle equals $\boldsymbol{E}_\infty$ even if the undisturbed field is a function of position on the scale of L.

The slip velocity on S^+ is given by (2.1) when $\kappa b \gg 1$. Because the particle does not conduct charge, the local electric field differs from $\boldsymbol{E}_\infty$. The tangential field $\boldsymbol{E}^s$ on S^+ is given by

$$\boldsymbol{E}^s = [\boldsymbol{e}_t\boldsymbol{e}_t + 2(-\boldsymbol{e}_b+\boldsymbol{e}_n)(-\boldsymbol{e}_n\sin\phi + \boldsymbol{e}_b\cos\phi)]\cdot\boldsymbol{E}_\infty \tag{2.20}$$

where ϕ is the polar angle measured from $\boldsymbol{e}_n$ in the plane perpendicular to the centreline direction. Because the hydrodynamic description is at the level of stokeslets, as defined

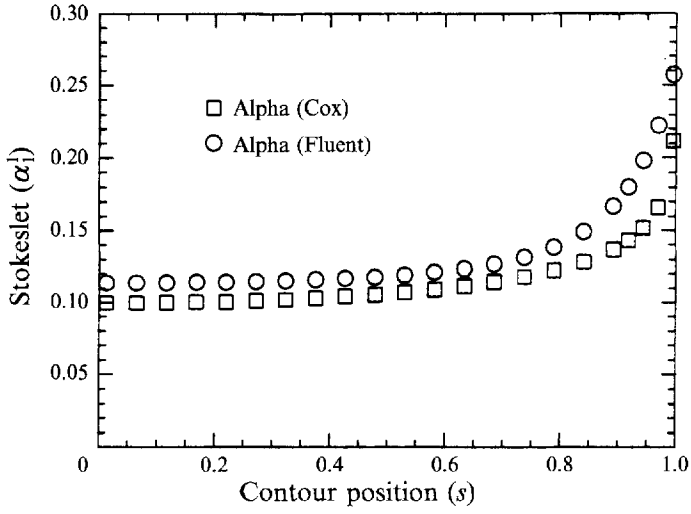

FIGURE 4. Comparison between Cox's theory (equations (2.14) and (2.16)) and a numerical solution of the Stokes equations (FLUENT) for a straight cylinder moving parallel to its axis (coordinate 1, see figure 3). $\epsilon = 0.1$.

in (2.11), the slip velocity that appears in (2.13) is a circumferential average at constant s. This average slip velocity is obtained by averaging $\boldsymbol{E}^s$ over ϕ; when combined with (2.1) the result is

$$\boldsymbol{u}(s) = -\left(\frac{DkT}{\eta e}\right)\zeta \boldsymbol{E}_\infty. \tag{2.21}$$

Both the zeta potential and applied electric field can be functions of s. In the examples in the next section we consider a constant electric field with ζ a function of s. In §4 the applied field is a quadratic function of position while ζ is a constant.

3. Non-uniformly charged particles in uniform fields

We demonstrate in this section the application of (2.13) to different geometries. The slip velocity is given by (2.21) with ζ a function of s but $\boldsymbol{E}_\infty$ a constant. The following distribution of zeta potential is assumed for many of the examples ($-1 < s < +1$):

$$\zeta(s) = \zeta_0 + \zeta_1 s + \zeta_2(3s^2 - 1), \tag{3.1}$$

where ζ_i are constants. We refer to these constants as the 'monopole' 'dipole' and 'quadrupole' moments for $i = 0$, 1 and 2. In this section the velocity vectors $\boldsymbol{U}$ and $\boldsymbol{\Omega}$ are made dimensionless by $(DkT/\eta e)\boldsymbol{E}_\infty$ and $(DkT/L\eta e)\boldsymbol{E}_\infty$, respectively, ζ is normalized by kT/e, and $\boldsymbol{E} = \boldsymbol{E}_\infty/E_\infty$.

3.1. *Straight particles*

There are three non-zero distinct stokeslet functions: α_1^1, α_2^2 and α_2^6, where the subscript '1' is the direction of the particle's axis and '2' is the direction defined by the component of $\boldsymbol{E}_\infty$ that is perpendicular to the axis (see figure 3). We use the brackets $\langle\,\rangle$ for integrals over s:

$$\langle f \rangle \equiv \frac{1}{2}\int_{-1}^{+1} f \,\mathrm{d}s.$$

The translational and angular velocities are determined from (2.13) to be

$$U_1 = \frac{\langle \alpha_1^1 \zeta \rangle}{\langle \alpha_1^1 \rangle} E_1, \tag{3.2a}$$

$$U_2 = \left[\frac{\langle \alpha_2^2 \zeta \rangle - \dfrac{\langle \alpha_2^6 \rangle \langle \alpha_2^6 \zeta \rangle}{\langle s\alpha_2^6 \rangle}}{\langle \alpha_2^2 \rangle - \dfrac{\langle \alpha_2^6 \rangle \langle s\alpha_2^2 \rangle}{\langle s\alpha_2^6 \rangle}} \right] E_2, \tag{3.2b}$$

$$\Omega_3 = \left[\frac{\langle \alpha_2^6 \zeta \rangle - \dfrac{\langle s\alpha_2^2 \rangle \langle \alpha_2^2 \zeta \rangle}{\langle \alpha_2^2 \rangle}}{\langle s\alpha_2^6 \rangle - \dfrac{\langle s\alpha_2^2 \rangle \langle \alpha_2^6 \rangle}{\langle \alpha_2^2 \rangle}} \right] E_2. \tag{3.2c}$$

For particles with fore–aft symmetry ($w(-s) = w(s)$), α_1^1 and α_2^2 are even functions of s and α_2^6 is an odd function of s. For such particles we have

$$U_1 = \frac{\langle \alpha_1^1 \zeta \rangle}{\langle \alpha_1^1 \rangle} E_1, \quad U_2 = \frac{\langle \alpha_2^2 \zeta \rangle}{\langle \alpha_2^2 \rangle} E_2, \quad \Omega_3 = \frac{\langle \alpha_2^6 \zeta \rangle}{\langle s\alpha_2^6 \rangle} E_2. \tag{3.3}$$

From (2.17) and (2.18) we have the following for cylinders and spheroids possessing the potential distribution of (3.1):

$$\text{Cylinder:} \quad \left.\begin{aligned} \frac{U_1}{E_1} &= \zeta_{ave} + \frac{2}{3[3-2\ln(4\epsilon)]}\zeta_2, \\ \frac{U_2}{E_2} &= \zeta_{ave} + \frac{2}{3[1-2\ln(4\epsilon)]}\zeta_2, \\ \frac{\Omega_3}{E_2} &= \zeta_1, \\ (\zeta_{ave} &= \zeta_0). \end{aligned}\right\} \tag{3.4}$$

$$\text{Spheroid:} \quad \left.\begin{aligned} \frac{U_1}{E_1} = \frac{U_2}{E_2} &= \zeta_{ave} + \tfrac{1}{4}\zeta_2; \quad \frac{\Omega_3}{E_2} = \zeta_1, \\ (\zeta_{ave} &= \zeta_0 - \zeta_2/4). \end{aligned}\right\} \tag{3.5}$$

ζ_{ave} is the area-average of the zeta potential.

The spheroid is an interesting case because to $O(\epsilon^2 \ln \epsilon)$ the stokeslets corresponding to translational motion (α_1^1 and α_2^2) are independent of s. Thus, even though the magnitude of the stokeslets differs between parallel and perpendicular motion, the electrophoretic mobility, U/E, is the same for both directions. For the cylinder, the electrophoretic mobility is greater for the perpendicular direction if ζ_0 and ζ_2 have the same sign. This behaviour is quite different from a cylinder undergoing sedimentation, in which case the mobility parallel to the axis approaches twice the value of the perpendicular case in the limit $\epsilon \to 0$. This example serves as a warning against applying the normal intuition developed for Stokes flows with uniformly distributed body forces, such as gravity, to phoretic transport where the driving forces are localized near

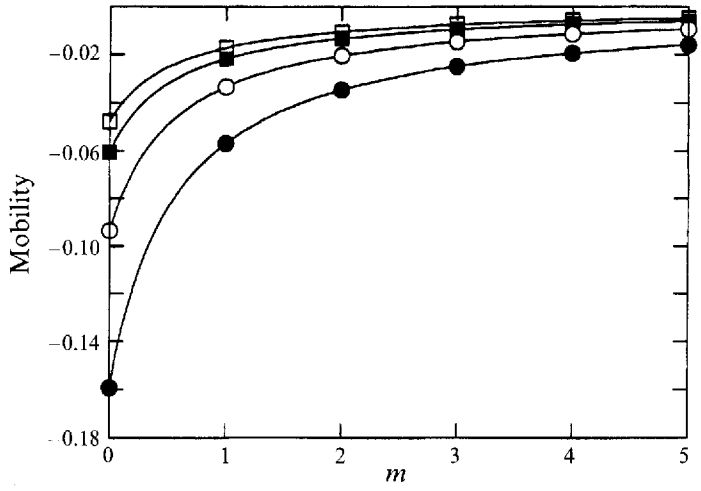

FIGURE 5. Electrophoretic mobility (U/E) of a straight circular cylinder with a periodic distribution of zeta potential as given in (3.6). The open symbols indicate the applied field is parallel to the axis of the cylinder and the filled symbols denote perpendicular alignment. Circles $\rightarrow \epsilon = 0.1$; squares $\rightarrow \epsilon = 0.01$. The mobility is made dimensionless by $(D/\eta)(kT/e)$. The curves represent equations (3.7)–(3.8).

the particle's surface. Another interesting feature of electrophoresis, which is apparent from (3.4) and (3.5), is that particles can move in an electric field even if the area-average zeta potential is zero, i.e. the particle is neutral. Other examples of neutral particles having a finite electrophoretic mobility are available (Fair & Anderson 1989; Anderson & Solomentsev 1994).

An interesting calculation is the mobility of a neutral cylinder with a periodic potential distribution:

$$\zeta(s) = \cos[(2m+1)\pi s], \tag{3.6}$$

where m is an integer. The mobilities ($M = U/E$, dimensionless) are determined by substituting this expression into (3.3) and using the stokeslet distributions given in (2.17). Plots of the mobilities versus m for a cylinder of $\epsilon = 0.01$ and 0.1 are shown in figure 5. The potential at the ends of the cylinder, in this case negative, dictates the direction of movement because the hydrodynamic resistance to motion is the greatest at the ends. We also note that magnitude of the mobility is greater for perpendicular motion than for parallel motion. In the limit of $m \rightarrow \infty$ the mobilities approach zero as expected. Both the parallel and perpendicular mobilities are fit extremely well by the following:

$$M(m) = \frac{M(0)}{1+1.8m}. \tag{3.7}$$

$M(0)$ increases in magnitude as ϵ increases. For the range $0.001 < \epsilon < 0.1$, $M(0)$ is approximated by the following expression:

$$M(0) = \frac{A}{\ln(\epsilon)+B}, \tag{3.8}$$

where $A = 0.22$, $B = 0$ for the parallel case, and $A = 0.21$, $B = 1$ for the perpendicular case.

For particles with fore–aft symmetry ($w(s) = w(-s)$) only the even moments of the zeta potential distribution affect translation while the odd moments cause rotation. Without this symmetry there will be coupling between the even and odd moments of the potential in (3.1), as indicated by (3.2); that is, ζ_2 would cause rotation and ζ_1 translation.

3.2. *Torus*

Johnson & Wu (1979) determined the stokeslet functions to $O(\epsilon^2 \ln \epsilon)$. The electrophoretic motion for the potential of (3.1) is cast in the form:

$$\left.\begin{aligned} \boldsymbol{U} &= \boldsymbol{M}_T \cdot \boldsymbol{E}, \quad \boldsymbol{\Omega} = \boldsymbol{M}_R \cdot \boldsymbol{E}, \\ \boldsymbol{M}_T &= \zeta_0 \boldsymbol{I} + \zeta_1 \boldsymbol{M}_T^{(1)} + \zeta_2 \boldsymbol{M}_T^{(2)}, \\ \boldsymbol{M}_R &= \zeta_1 \boldsymbol{M}_R^{(1)} + \zeta_2 \boldsymbol{M}_R^{(2)}. \end{aligned}\right\} \tag{3.9}$$

The orientation of the torus relative to the fixed Cartesian axes (1, 2, 3) is shown in figure 3. The velocity of the particle was determined from (2.13) and (2.19). The non-zero mobilities are given below.

$$\left.\begin{aligned} M_T^{(1)}(1,3) = M_T^{(1)}(3,1) &= \frac{17 - 16\ln\left(\dfrac{8}{\pi\epsilon}\right)}{2\pi\left[-7 + 2\ln\left(\dfrac{8}{\pi\epsilon}\right)\right]}, \\ M_T^{(2)}(1,1) = -M_T^{(2)}(3,3) &= \frac{3}{\pi} M_T^{(1)}(1,3), \\ M_R^{(1)}(2,3) = -\tfrac{1}{2} M_R^{(1)}(3,2) &= \frac{1}{\pi}, \\ M_R^{(2)}(1,2) = -2M_R^{(2)}(2,1) &= -\frac{12}{\pi^2}. \end{aligned}\right\} \tag{3.10}$$

A novel result is the orthogonal motion resulting from the dipole coefficient ζ_1; a field oriented in the 3 direction couples with the dipole along the contour to move the torus in the 1 direction. To show that orthogonal motion is possible with other particles of relatively simple geometry, figure 6 shows a dumb-bell formed by two equal-size spheres connected by an infinitely thin, rigid rod. Both spheres have a quadrupole moment of the same magnitude $|\zeta_2|$ (see (3.1) and set $s = \cos\theta$) but opposite sign and orientation. If hydrodynamic interactions between the spheres are neglected, then the velocity of the dumb-bell in an electric field can be determined from the theory for a single non-uniformly charged sphere (Anderson 1985). In this case the dumb-bell moves perpendicular to the electric field at a speed equal to $(3/10)\,\zeta_2 E \sin 2\psi$ where ψ is the angle between the axis of the quadrupole and the field.

These examples are meant to illustrate the relative simplicity of the theory. The hydrodynamic model of Cox gives an explicit relationship that allows direct calculation of the stokeslet distribution for any $w(s)$ and straight or curved contours ($\boldsymbol{X}_0(s)$). Given the simplified nature of the model (for example, a 'smooth' slender surface) and the restriction that $\kappa b_0 \gg 1$, it is doubtful that a more accurate calculation of the stokeslet density can be justified, at least at the level of our analysis.

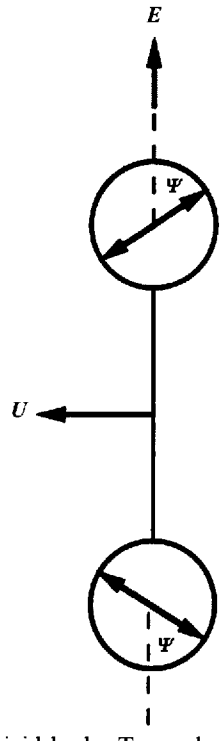

FIGURE 6. Perpendicular motion of a rigid body. Two spheres with quadrupole moments of equal magnitude but opposite sign whose axes are oriented in the 1–2 plane as shown by the arrows within the spheres. The rigid dumb-bell moves perpendicular to the applied field E at velocity $U = (3/10)[\sin(2\Psi)]\zeta_2 E$ where ζ_2 is the quadrupole moment of the top sphere.

4. Uniformly charged slender particles in non-homogeneous fields

In the examples of the previous section the undisturbed electric field is taken to be independent of position. We now consider a uniformly charged ($\zeta = \zeta_0$) particle in a spatially varying electric field $E_\infty(x)$. A uniformly charge sphere obeys Smoluchowski's equation (2.2) for any field as long as $\nabla \cdot E_\infty = 0$ (Anderson 1985). This is not true for slender bodies; ∇E_∞ causes rotation of slender particles while $\nabla\nabla E_\infty$ affects the translational velocity, as shown below.

Consider a straight particle with fore–aft symmetry. The variables are non-dimensionalized as in the previous section, and ∇ is normalized by L. The unit vector e gives the direction of the centreline axis ($e = e_t$). Subscript 1 corresponds to the direction along e and (2, 3) designate the directions perpendicular to e. The translational and rotational velocities are obtained from (2.13):

$$U_1 = -\frac{\langle \alpha_1^1 u_1 \rangle}{\langle \alpha_1^1 \rangle}, \quad U_2 = -\frac{\langle \alpha_2^2 u_2 \rangle}{\langle \alpha_2^2 \rangle}, \quad \Omega_3 = -\frac{\langle \alpha_2^6 u_2 \rangle}{\langle s\alpha_2^6 \rangle}, \tag{4.1}$$

with analogous terms for U_3 and $-\Omega_2$ ($2 \to 3$, $6 \to 5$). The slip velocity is given by (2.21) with E a function of position ($E = E_\infty / E_{\infty_0}$). The Taylor expansion of E about the centre of the particle (X_p) approximates the field along the contour of the particle:

$$E(s) = E(X_p) + se \cdot \nabla E + \tfrac{1}{2} s^2 ee : \nabla\nabla E. \tag{4.2}$$

Combining (4.1) and (4.2) gives the velocity of the particle:

$$U = \zeta_0 [E(X_p) + \tfrac{1}{6} ee : \nabla\nabla E], \tag{4.3a}$$

$$\Omega = \zeta_0 e \times (e \cdot \nabla E). \tag{4.3b}$$

Higher-order gradients are neglected. The $O(\nabla\nabla \boldsymbol{E}_\infty)$ term was obtained by assuming the translational stokeslet function is constant, which is correct at $O((\ln\epsilon)^{-1})$ for general slender particles; thus, this term has an error of $O((\ln\epsilon)^{-2})$ associated with it even if $\kappa b_0 \gg 1$. Equation (4.3) applies to any straight, slender particle having fore–aft symmetry, regardless of the radius profile $w(s)$.

An example of a non-homogeneous field is ionic conduction in an electrolyte solution through a circular hole in an insulating wall, as shown in figure 7. This situation would arise, for example, in the electrophoretic transport of particles across a porous membrane. Newman (1966) and Kelman (1965) give solutions to Laplace's equation for such geometries.

An interesting question is whether or not the converging field lines into the entrance of the hole can align slender particles to an extent that allows them to enter the hole even if the particle length exceeds the pore diameter? The goal is to estimate the critical electrical current through the hole, I_c, above which a majority of the particles in a suspension would be sufficiently aligned. This problem is conceptually related to the analysis of deformation of linear polymer chains in extensional flow through a small aperture (Daoudi & Brochard 1978).

The field outside the pore at a distance r (non-dimensionalized by L) from the hole much greater than the radius of the hole (a) is approximated by the field for conduction into a point source:

$$\boldsymbol{E}_\infty = -\frac{I}{2\pi r^3 L^2 K}\boldsymbol{r}, \tag{4.4}$$

where I is the total current into the hole and K is the specific conductivity of the electrolyte solution. After the field is expanded about the centre of the particle ($\boldsymbol{r} = \boldsymbol{r}_p$) and then substituted into (4.3) with terms of $O(\nabla\nabla \boldsymbol{E}_\infty)$ and higher neglected, the following relations are obtained:

$$\frac{\mathrm{d}r_p}{\mathrm{d}t} = -\frac{\zeta_0 I}{2\pi r_p^2 L^2 K}, \tag{4.5a}$$

$$\frac{\mathrm{d}(\cos\theta)}{\mathrm{d}t} = \frac{3\zeta_0 I}{2\pi r_p^3 L^3 K}\cos\theta\sin^2\theta, \tag{4.5b}$$

where θ is the solid angle between $\boldsymbol{e}$ and $-\boldsymbol{r}_p$. If terms of $O(\nabla\nabla \boldsymbol{E}_\infty)$ where included then there would be a small drift of the particle perpendicular to the $\boldsymbol{r}_p$ direction (in the direction of $-\boldsymbol{e}$) and (4.5a) would be slightly modified; however, use of the approximation (4.4) does not justify inclusion of this secondary migration term. The trajectory is found by combining the above two expressions:

$$\frac{\tan\theta}{\tan\theta_0} = \left(\frac{r}{r_{p0}}\right)^3, \tag{4.6}$$

where the subscript 0 denotes the initial condition.

Equation (4.6) seems to indicate that the current, and hence the applied potential difference across the hole, has no influence on the trajectory. In fact, the effect of the current is in the initial condition (r_{p0}, θ_0). The relations (4.5) were derived neglecting Brownian rotation of the particle, which is a good assumption only when the rotational Péclet number (Pe_r) exceeds one. This requirement gives us a criterion for fixing the initial condition; that is, r_{p_0} is the position of the particle when $Pe_r = \Omega/D_r = 1$ where Ω is a characteristic angular velocity and D_r is the rotational diffusion coefficient. For

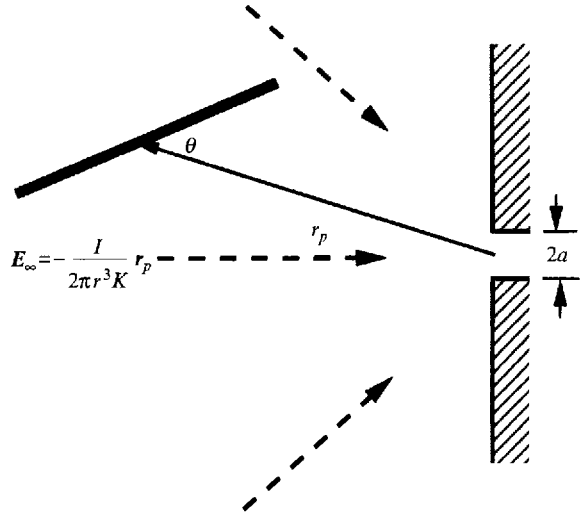

FIGURE 7. Uniformly charged, straight particle in a non-homogeneous electric field caused by conduction of current (I) through a circular hole in an insulating wall. The current (shown by arrows with broken lines) is carried by the ions of the electrolyte in the liquid.

straight slender particles the rotational diffusion coefficient can be expressed in the form

$$D_r = \frac{kT}{A\pi\eta L^3} g(\epsilon), \tag{4.7}$$

where A and $g(\epsilon)$ depend on the profile $w(s)$. The value of Ω is obtained from the constant parameters in (4.5b). Setting $Pe_r = 1$ gives

$$r_{p0} = \left[\frac{3AD}{2g(\epsilon)}\left(\frac{kT/e)\,\zeta_0 I}{Ke}\right)\right]^{1/3}. \tag{4.8}$$

If we assume a random distribution of particle orientations at this starting position then $\langle \cos^2\theta_0 \rangle = \frac{1}{3}$ and hence $\theta_0 \approx 55°$.

We are interested in whether or not the particle is aligned with the axis of the hole when $r_p = L$. The critical alignment for the particle to enter the hole is approximated by

$$L \sin\theta_c \approx a. \tag{4.9}$$

Combining this requirement with (4.6) and (4.8) and assuming $L \gg a$ and $\tan\theta_0 = \sqrt{2}$ gives the following result for the critical current:

$$I_c = \left(\frac{8}{9}\right)^{1/2}\left[\frac{g(\epsilon)}{AD}\left(\frac{eK}{\zeta_0}\right)\right]\frac{L}{a}. \tag{4.10}$$

Note that ζ_0 is non-dimensionalized by kT/e while the other parameters (D, e, K, L, a) are dimensional. If the current conducted through the hole is much smaller than I_c then very few of the particles should be sufficiently aligned to pass through, while a majority should pass if $I \gg I_c$.

As expected, the critical current is higher for smaller pores. To estimate a typical magnitude of I_c, consider a 0.1 molar solution of potassium chloride in water at 25 °C ($D = 6.94 \times 10^{-10}$ Coul/V·m, $\eta = 8.94 \times 10^{-4}$ kg/m·s, and $K = 1.288$ Coul/V·m·s). ζ_0 is taken equal to 1 ($kT/e = 0.0257$ V). For a spheroid $A = \frac{8}{3}$ and $g(\epsilon) = [2\ln(2\epsilon^{-1}) - 1]$. Substituting $\epsilon = 0.01$ into (4.10) yields

$$I_c = 1.04 \times 10^{-9}(L/a) \quad \text{Coul s}^{-1}. \tag{4.11}$$

The electrical potential drop across a hole in a plane of zero thickness equals $I/2Ka$ (Newman 1966). Taking half of this as the critical potential ($\Delta\Phi_c$) that must be applied across the solution on one side of the barrier, (4.11) gives

$$\Delta\Phi_c = 2.01 \times 10^{-10}(L/a^2)\text{V}. \tag{4.12}$$

The critical potential drop for a hole of radius 0.1 μm and $L = 1$ μm would be only 20 mV. A test for the critical current (or potential) is possible by applying a voltage across a microporous membrane separating two reservoirs, one of which contains a dilute suspension of the slender particles, and measuring the current required to drive the particles through the small pores.

The above example indicates that a linear variation in the field can produce significant alignment of uniformly charged slender particles. Equations (4.1) could also be used to determine the velocity of a straight non-uniformly charged particle in a non-homogeneous electric field. Furthermore, these relations are expressed in terms of slip velocity so that they can be applied to other phoretic transport phenomena such as diffusiophoresis.

5. Summary

The equations (2.13) allow calculation of the translational and angular velocities of a slender particle when the slip velocity is specified along the centreline of the particle. The variation of $\boldsymbol{u}$ could result from a non-uniform surface property of the particle, such as the zeta potential, or a non-uniform applied field. These two cases are considered in §§3 and 4. This theory applies to any linear phoretic process (Anderson 1989) as long as the thickness of the fluid region comprising the 'interface' between the particle surface and surrounding fluid, here taken to be the Debye screening length, is small compared to the cross-section radius of the particle. In the examples presented here we have used Cox's theory (1970) for the stokeslets along a circular cylinder or the more exact results available for a prolate spheroid and torus. Cox's method for determining $\alpha(s)$ is quite useful when centreline geometries more complicated than the torus are considered, for example, a helix.

The interesting feature of electrophoresis of slender particles is that the zeta potential of the portions of the particle that are more hydrodynamically 'exposed', such as the ends of a cylinder, have more influence than the hydrodynamically screened regions. This is one reason that neutral particles (i.e. particles with a zero area-average of ζ) can have a significant translational velocity when placed in an electric field. We have applied the model of a circular cylinder to compute the electrophoretic mobility of a chain of equal size spheres each of which could have different zeta potentials (Anderson & Solomentsev 1994). Essentially the spheres at the ends of the chain dictate the direction and magnitude of the electrophoretic velocity.

The penalty for applying the Lorentz reciprocal theorem at the outer edge of the double layer is that the results for $\boldsymbol{U}$ and $\boldsymbol{\Omega}$ are valid at $O((\ln\epsilon)^{-1})$ only when $\kappa b_0 \gg \ln(\epsilon)$. This is because the primary source of error in (2.7) is in approximating the velocity $\boldsymbol{v}^*$ at S^+ by its value on S^p. The displacement between these two surfaces is $O(\kappa^{-1})$. Since the velocity gradient for a slender body is $O((b_0 \ln\epsilon)^{-1})$,

$$(\boldsymbol{v}^*)_{S^+} = (\boldsymbol{v}^*)_{S^p}\left[1 - O\left(\frac{1}{\kappa b_0 \ln\epsilon}\right)\right]. \tag{5.1}$$

Therefore, the error in (2.7) is $O((\kappa b_0 \ln\epsilon)^{-1})$, and hence the error in (2.13) is also $O((\kappa b_0 \ln\epsilon)^{-1})$. The consequence of the requirement $\kappa b_0 \gg \ln(\epsilon)$ is that (2.13) is

probably only quantitatively accurate to $O((\ln\epsilon)^{-1})$ for colloidal slender bodies (bundles of chain-like molecules, aggregates of colloidal particles) and not for single macromolecular chains such as polyelectrolytes.

This research was supported by NASA Grant NANAG8-964.

REFERENCES

ACRIVOS, A., JEFFREY, D. J. & SAVILLE, D. A. 1990 Particle migration in suspensions by thermocapillary or electrophoretic motion. *J. Fluid Mech.* **212**, 95.

ANDERSON, J. L. 1985 Effect of nonuniform zeta potential on particle movement in electric fields. *J. Colloid Interface Sci.* **105**, 45.

ANDERSON, J. L. 1989 Colloid transport by interfacial forces. *Ann. Rev. Fluid Mech.* **21**, 61.

ANDERSON, J. L. & SOLOMENTSEV, Y. 1994 Electrophoresis of nonuniformly charged chains. In *Macro-ion Characterization: From Dilute Solutions to Complex Fluids* (ed. K. S. Schmitz). American Chemical Society Symposium Series, no. 548.

BATCHELOR, G. K. 1970 Slender-body theory for particles of arbitrary cross-section in Stokes flow. *J. Fluid Mech.* **44**, 419.

COLE, J. D. 1968 *Perturbation Methods in Applied Mathematics.* Waltham, Massachusetts: Blaisdell.

COX, R. G. 1970 The motion of long slender bodies in a viscous fluid. Part 1. General theory. *J. Fluid Mech.* **44**, 791.

DAOUDI, S. & BROCHARD, F. 1978 Flows of flexible polymer solutions in pores. *Macromolecules* **11**, 751.

DUKHIN, S. S. & DERJAGUIN, B. V. 1974 *Surface and Colloid Science*, vol. 7 (ed. E. Matijevic). Wiley.

FAIR, M. C. 1990 Electrophoresis of nonspherical and nonuniformly charged colloidal particles. PhD thesis, Carnegie Mellon University.

FAIR, M. C. & ANDERSON, J. L. 1989 Electrophoresis of nonuniformly charged ellipsoidal particles. *J. Colloid Interface Sci.* **127**, 388.

FAIR, M. C. & ANDERSON, J. L. 1990 Electrophoresis of dumbbell-like colloidal particles. *Intl J. Multiphase Flow* **16**, 663, 1131.

FAIR, M. C. & ANDERSON, J. L. 1992 Electrophoresis of heterogeneous colloids: doublets of dissimilar particles. *Langmuir* **8**, 2850.

HAPPEL, J. & BRENNER, H. 1973 *Low Reynolds Number Hydrodynamics.* Noordhoff.

HENRY, D. C. 1931 The cataphoresis of suspended particles. Part I. The equation of cataphoresis. *Proc. R. Soc. Lond.* A **133**, 106.

HUNTER, R. J. 1981 *Zeta Potential in Colloid Science.* Academic.

JOHNSON, R. E. 1980 An improved slender-body theory for Stokes flow. *J. Fluid Mech.* **99**, 411.

JOHNSON, R. E. & WU, T. Y. 1979 Hydrodynamics of low-Reynolds-number flow. Part 5. Motion of a slender torus. *J. Fluid Mech.* **95**, 263.

KELLER, J. B. & RUBINOW, S. I. 1976 Slender-body theory for slow viscous flow. *J. Fluid Mech.* **75**, 705.

KEH, H. J. & CHEN, S. B. 1993 Diffusiophoresis and electrophoresis of colloidal cylinders. *Langmuir* **9**, 1142.

KEH, H. J. & YANG, F. R. 1991 Particle interactions in electrophoresis. IV. Motion of arbitrary three-dimensional clusters of spheres. *J. Colloid Interface Sci* **145**, 362.

KELMAN, R. B. 1965 Steady state diffusion through a finite pore with an infinite reservoir. *Bull. Math. Biophics* **27**, 57.

MANGELSDORF, C. S. & WHITE, L. R. 1992 The electrophoretic mobility of a spherical colloid in an oscillating electric field. *J. Chem. Soc. Faraday Trans.* **88**, 3567.

MELCHER, J. R. 1981 *Continuum Electromechanics.* MIT Press.

NEWMAN, J. S. 1966 Resistance for flow of current to a disk. *J. Electrochem. Soc.* **113**, 501.

O'BRIEN, R. W. 1983 The solution of the electrokinetic equations for colloidal particles with thin double layers. *J. Colloid Interface Sci.* **92**, 204.

O'BRIEN, R. W. 1990 The electroaccoustic equations for a colloidal suspension. *J. Fluid Mech.* **212**, 81.

O'BRIEN, R. W. & WHITE, L. R. 1978 Electrophoretic mobility of a spherical colloidal particle. *J. Chem. Soc. Faraday Trans.* **74** (2), 1607.

O'BRIEN, R. W. & WARD, D. N. 1988 The electrophoresis of a spheroid with a thin double layer. *J. Colloid Interface Sci.* **121**, 402.

PAWAR, Y. 1993 Electrophoresis of heterogencously charged colloidal particles. PhD thesis, Carnegie Mellon University.

RUSSEL, W. B., SAVILLE, D. A. & SCHOWALTER, W. R. 1989 *Colloidal Dispersions.* Cambridge University Press.

SAVILLE, D. A. 1977 Electrokinetic effects with small particles. *Ann. Rev. Fluid Mech.* **9**, 321.

SHERWOOD, J. D. 1982 Electrophoresis of rods. *J. Chem. Soc. Faraday Trans. 2* **78**, 1091.

SOLOMENTSEV, Y., PAWAR, Y. & ANDERSON, J. L. 1993 Electrophoretic mobility of nonuniformly charged spherical particles with polarization of the double layer. *J. Colloid Interface Sci.* **158**, 1.

TEUBNER, M. 1982 The motion of charged colloidal particles in electric fields. *J. Chem. Phys.* **76**, 5564.

YOON, B. J. 1991 Electrophoretic motion of spherical particles with a nonuniform charge distribution. *J. Colloid Interface Sci.* **142**, 575.

YOON, B. J. & KIM, S. 1989 Electrophoresis of spheroidal particles. *J. Colloid Interface Sci.* **128**, 275.